LABORATOIRE
DE
PHYSIQUE CORPUSCULAIRE

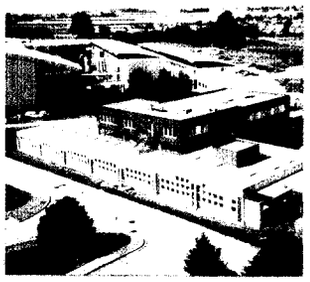

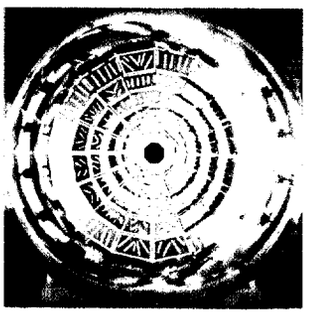

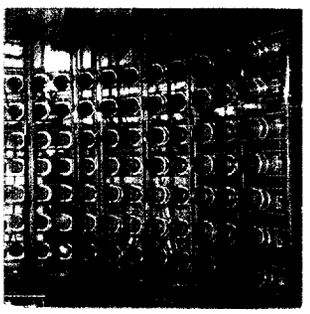

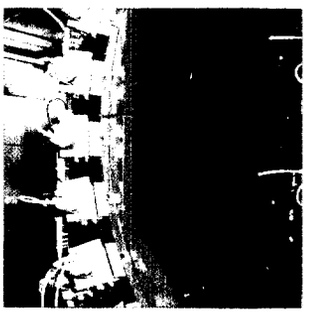

# Angular momentum transfer in the Xe+Sn collisions

E. Genouin-Duhamel, J.C. Steckmeyer, E. Vient, J. Colin, D. Durand, G. Auger, C.O. Bacri, N. Bellaize, F. Bocage, B. Borderie, R. Bougault, R. Brou, P. Buchet, J.L. Charvet, A. Chbihi, D. Cussol, R. Dayras, A. Demeyer, D. Doré, J.D. Frankland, E. Galichet, E. Gerlic, D. Guinet, P. Lautesse, J.L. Laville, J.F. Lecolley, R. Legrain, N. Le Neindre, O. Lopez, M. Louvel, A.M. Maskay, L. Nalpas, A.D. N'Guyen, M. Pârlog, J. Péter, E. Plagnol, M.F. Rivet, E. Rosato, F. Saint-Laurent, S. Salou, M. Stern, G. Tabacaru, B. Tamain, L. Tassan-Got, O. Tirel, C. Volant, J.P. Wieleczko

(INDRA Collaboration)

March 1999 LPCC 99-09

Contribution given at the xxxvii th International Winter Meeting on Nuclear Physics, Bormio, Italy, 25-30 January, 1999.

CENTRE NATIONAL DE LA RECHERCHE SCIENTIFIQUE

INSTITUT NATIONAL
DE PHYSIQUE NUCLÉAIRE ET DE PHYSIQUE DES PARTICULES

INSTITUT DES SCIENCES DE LA MATIÈRE ET DU RAYONNEMENT

UNIVERSITÉ DE CAEN

- U.M.R.6534 -
ISMRA - 6, Boulevard Maréchal Juin - 14050 CAEN CEDEX - FRANCE

Téléphone : 02 31 45 25 00 - Télécopie : 02 31 45 25 49
Internet : http://caeinfo.in2p3.fr

# Angular momentum transfer in the Xe+Sn collisions [1]

E. Genouin-Duhamel[a], J.C. Steckmeyer[a], E. Vient[a], J. Colin[a], D. Durand[a], G. Auger[b], C.O. Bacri[c], N. Bellaize[a], F. Bocage[a], B. Borderie[c], R. Bougault[a], R. Brou[a], P. Buchet[d], J.L. Charvet[d], A. Chbihi[b], D. Cussol[a], R. Dayras[d], A. Demeyer[e], D. Doré[d], J.D. Frankland[c,2], E. Galichet[e], E. Gerlic[e], D. Guinet[e], P. Lautesse[e], J.L. Laville[b], J.F. Lecolley[a], R. Legrain[d], N. Le Neindre[a], O. Lopez[a], M. Louvel[a], A.M. Maskay[e], L. Nalpas[d], A.D. N'Guyen[a], M. Pârlog[f], J. Péter[a], E. Plagnol[c], M.F. Rivet[c], E. Rosato[g], F. Saint-Laurent[b,3], S. Salou[b], M. Stern[e], G. Tăbăcaru[c,f], B. Tamain[a], L. Tassan-Got[c], O. Tirel[b], C. Volant[d] and J.P. Wieleczko[b].

**INDRA Collaboration**

[a] *Laboratoire de Physique Corpusculaire, IN2P3-CNRS, ISMRA et Université, F-14050 Caen Cedex, France*

[b] *Grand Accélérateur National d'Ions Lourds, DSM-CEA/IN2P3-CNRS, BP 5027, F-14076 Caen Cedex 5, France*

[c] *Institut de Physique Nucléaire, IN2P3-CNRS, BP 1, F-91406 Orsay Cedex, France*

[d] *DAPNIA/SPhN, CEA/Saclay, Orme des Merisiers, F-91191 Gif-sur-Yvette Cedex, France*

[e] *Institut de Physique Nucléaire, IN2P3-CNRS et Université, F-69622 Villeurbanne Cedex, France*

[f] *National Institute for Physics and Nuclear Engineering, RO-76900 Bucharest-Măgurele, Romania*

[g] *Dipartimento di Scienze Fisiche e Sezione INFN, Università di Napoli "Federico II", I-80126 Napoli, Italy*

**Abstract**

The angular momentum transferred into intrinsic spin to the projectile-like fragment in the $^{129}$Xe+$^{nat}$Sn peripheral collisions at bombarding energies between 25 and 50 MeV per nucleon has been deduced from the angular distributions and kinetic energies of the emitted light charged particles (p, d, t, $^3$He and $\alpha$). The spin values decrease with the violence of the collision. Larger spin values are observed at the lowest bombarding energy. Data are compared with the predictions of transport models. They reproduce the data in a quantitative way indicating that large spin values are transferred to the projectile-like fragment in the course of the collision. The role of the particles emitted at mid-velocity is discussed.

[1] Experiment performed at Ganil

[2] Present address: Institut de Physique Nucléaire, F-69622 Villeurbanne Cedex, France

[3] Permanent address: DRFC/STEP CEA/Cadarache, F-13108 Saint-Paul-lez-Durance, France

# 1 Introduction

In the course of a collision between projectile and target nuclei, energy and angular momentum are dissipated into various degrees of freedom. In particular a fraction of the total angular momentum is transferred into intrinsic spins to the residual nuclei.

At bombarding energies smaller than 10 MeV/nucleon, the angular momentum transfer (AMT) was studied by means of different techniques all based on the measurement of the decay properties of the nuclei: multiplicity and angular distributions of $\gamma$-rays [1] or angular distributions of light charged particles (LCP) [2] or fission fragments in case of a heavy nucleus [3]. Many experiments have been performed in this energy range. Broadly speaking large spin values are transferred to the nuclei in the interaction (several tenths of $\hbar$ units) and a strong alignment of AMT is observed along the normal to the reaction plane [4]. Statistical [5] and transport [6] models are equally successful in describing the data.

At bombarding energies higher than 100 MeV/nucleon the participant-spectator scenario predicts little interaction between projectile and target remnants and the rest of the nucleons. Therefore a strong correlation between AMT and the spectators is not expected. One measurement performed at several hundreds of MeV per nucleon indicates that the projectile-like fragment (PLF) is left at the end of the interaction without spin suggesting that different reaction mechanisms for AMT could prevail at these energies [7].

At intermediate bombarding energies ($10 < E_{bomb} < 100$ MeV/nucleon) a few measurements are available [8]. Their interpretation is more complex than in the low energy case as this transition regime is dealing with excited nuclei emitting several particles. Studying AMT in this energy domain can provide a better understanding of the following points: (i) the real nature of the underlying reaction mechanism of AMT (exchange of nucleons [6], excitation of collective modes [5, 9, 10]), (ii) the equilibration time for the dissipation of the angular momentum in heavy ion collisions [11], (iii) the nuclear viscosity of the nuclear matter (tangential friction forces) [12] and (iv) the influence of angular momentum on the deexcitation of hot nuclei [13].

This contribution reports on the study of the angular momentum transferred into the PLF in the $^{129}$Xe+$^{nat}$Sn collisions at 25, 39 and 50 MeV/nucleon bombarding energies using information from angular distributions and kinetic energies of the emitted LCP's.

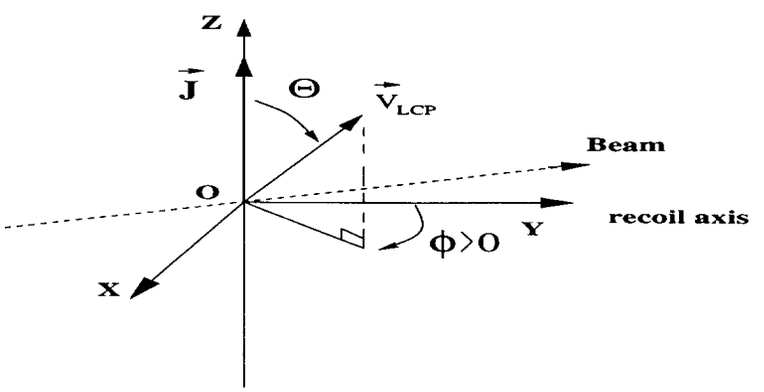


Figure 1: Rest frame of the emitter. $\Theta$ and $\Phi$ are the out-of-plane and in-plane angles, respectively. The reaction plane is defined by the beam direction and that of the recoil of the emitter (Y-axis). The spin is aligned along the normal to the reaction plane (Z-axis).

## 2 Experimental angular distributions of LCP's

The angular distribution of emitted LCP's in the rest frame of the emitter is given by the following relation: $W(\Theta) \approx \exp(-\cos^2(\Theta)/2\sigma^2)$ where $\Theta$ is the out-of-plane angle with respect to the spin axis (see fig. 1). The width $\sigma$ can be expressed as:

$$\sigma^2 = \frac{IT}{\hbar^2 J^2} \times \frac{I + \mu R^2}{\mu R^2} \tag{1}$$

where J is the spin of the emitter, I and T the moment of inertia and the temperature of the residual nucleus and $\mu R^2$ the relative moment of inertia of the configuration.

The angular distribution $W(\Theta)$ is anisotropic with a maximum at $\Theta = 90°$ in the reaction plane. The anisotropy increases with the increase of the spin of the emitter and with the increase of the particle mass, it decreases with the increase of the temperature. From the width of the angular distribution the spin of the nucleus can be extracted, provided that T is known (see eq. 1).

The $^{129}$Xe+$^{nat}$Sn reaction has been measured with the Indra experimental setup [14, 15]. Binary dissipative collisions are associated with the largest part of the reaction cross-section. In between target and projectile sources, data exhibit an emission of LCP's in the mid-velocity region [16]. To avoid this mid-velocity contribution only particles emitted in the forward hemisphere of the PLF will be considered in the analysis.

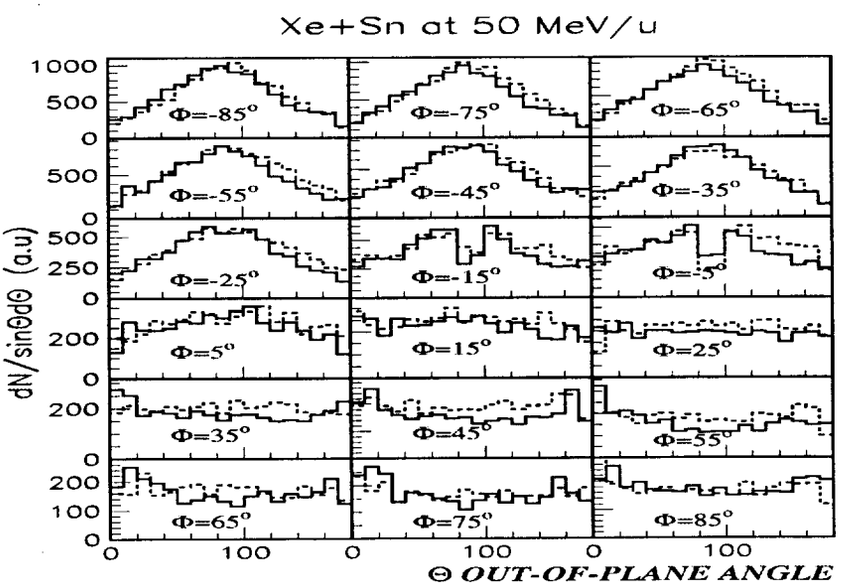


Figure 2: Out-of-plane angular distributions shown as a function of the in-plane angle. These data concern $\alpha$ particles emitted from PLF's produced in events with $50 < E_\perp < 100$ MeV. Solid lines are the data, dashed lines are results of a simulation (see text).

The velocity of the emitter (the primary PLF) is reconstructed from the velocities of all fragments with charge greater than or equal to 3 [17, 18] detected in the forward hemisphere in the center of mass of the reaction. Once the source velocity is known, the $\Theta$ and $\Phi$ angles are calculated and the angular distribution built. Solid lines in fig. 2, show as a function

of the $\Phi$ in plane angle, the out of plane angular distributions of $\alpha$ particles emitted by PLF's produced in events having a $E_\perp$ transverse energy between 50 and 100 MeV. The transverse energy is calculated event by event with all LCP's with charge 1 and 2 [16]. Anisotropic angular distributions with a maximum at $\Theta = 90°$ are observed at negative in plane angles while flat distributions are observed at positive in plane angles. Such a behaviour is unexpected as an anisotropic shape should also be observed for positive in-plane angles.

Using the transverse energy as a selector of the violence of the collision results in a mixing of events which do not have the same characteristics. In particular they can be associated with different deflection angles for the PLF. Indeed it is well known that the production cross-section of PLF's in heavy ion collisions is peaked at very forward angles. For a PLF detected at a given angle $\alpha_{det}$, the primary PLF should have been emitted at an angle $\alpha_{prim} < \alpha_{det}$. The $d\sigma/d\Omega$ cross-section favors such configurations with respect to other configurations in which the primary PLF is emitted at an angle $\alpha_{prim} > \alpha_{det}$. According to the momentum conservation the LCP's are emitted, with respect to the detected PLF, on the other side of the primary PLF or on the other side of the beam (as these two directions nearly coincide). This explains the excess of particles at $\Phi \approx$ -90° and the lack of particles at $\Phi \approx 90°$ (solid lines in fig. 2). In case of an isotropic $d\sigma/d\Omega$, identical out-of-plane angular distributions are observed, as it should, for positive and negative in-plane angles (that has been checked with a simulation).

Therefore the spin values cannot be accessed from the experimental widths of the out-of-plane angular distributions as they have to be unfolded from the angular distributions of the primary PLF. The proper way to extract the spin value from the data would be to perform calculations gated by the experimental setup and reproducing all observables: charge, energy, multiplicity and angular distributions. At present time such a procedure is unthinkable. Instead a simple simulation has been developed.

# 3 Simulation of angular distributions of LCP's

The ingredients of the simulation are the following ones: (i) the primary PLF is produced according to given charge, velocity and angular distributions, (ii) the PLF emits only one type of particle with energy and multiplicity distributions taken from the experiment (doing so can be considered as a substitute for simulating the whole deexcitation chain), (iii) the simulation is then filtered by the experimental setup, and (iv) the simulation is done again till the charge, velocity and angular distributions of the simulated detected PLF reproduce the corresponding experimental distributions, this being done by varying the primary distributions of step (i).

Once the simulation reproduces the characteristics of the detected PLF, the $\sigma$ parameter (eq. 1) is varied and the best value is the one which minimizes the difference between the simulated and experimental LCP angular distributions [19].

In fig. 2 are displayed the simulated and experimental distributions of $\alpha$ particles (50 $< E_\perp <$ 100 MeV). As seen the flat distributions observed at positive in-plane angles are now quite well reproduced. From this comparaison we extract a value for the width of the angular distributions of $\sigma = 0.85$. With a temperature of 4.8 MeV (cf. table 1) and an average mass of the residual nucleus of 109 a.m.u., a spin value of $(43 \pm 13)\ \hbar$ is deduced, the uncertainty being mainly due to the uncertainties on the average mass of the emitter

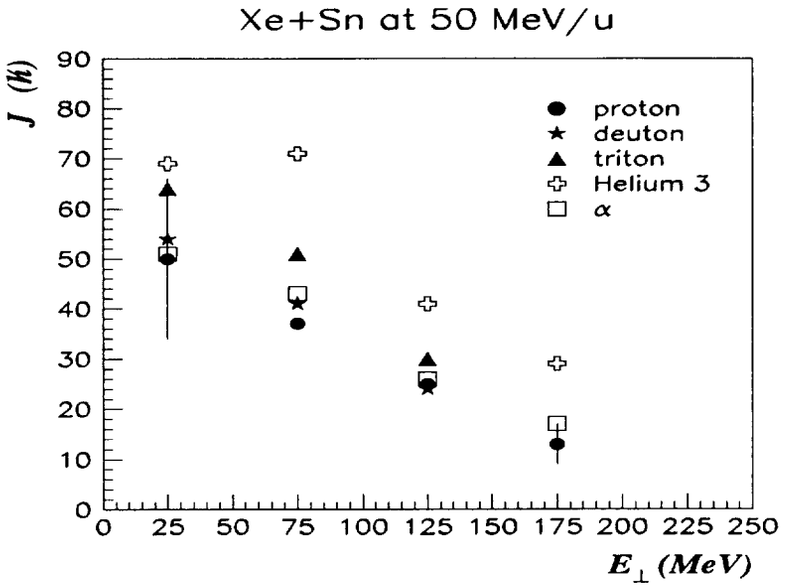


Figure 3: Apparent spin values of PLF deduced from the angular distributions of p, d, t, $^3$He and $\alpha$ as a function of the transverse energy. Typical uncertainties are plotted.

and on its temperature.

This simulation has been performed for all types of LCP's (p, d, t, $^3$He and $\alpha$) and for several bins in $E_\perp$. All results are shown in fig. 3.

# 4 Kinetic energy spectra of LCP's

The average kinetic energy of a particle emitted by a spherical nucleus in rotation [20] is given by the following relation: $<E> \approx B + 2T + T \sin^2(\Theta) / 2\sigma^2$ where the two first terms of the right hand side are the Coulomb barrier for the emission of the particle and the contribution from the thermal energy. The third term is an extra energy driven by the angular momentum. It is maximum in the reaction plane at $\Theta = 90°$. The difference $\Delta<E>$ between the energies measured at $\Theta = 90°$ and $0°$ allows for the determination of the spin of the nucleus according to the following relation:

$$J \approx \frac{I}{\hbar}\sqrt{\frac{2\,\Delta<E>}{\mu R^2}} \qquad (2)$$

The advantage of this method with respect to the previous one is that the estimation of the spin is independent of the temperature of the residual nucleus.

The kinetic energy spectra of LCP's have been built as a function of the out-of-plane angle. The evolution of the mean kinetic energy shows a maximum in the reaction plane as expected. The $\Delta<E>$ values are derived from the data with a fitting procedure. Spin values are then deduced for all types of particles and different $E_\perp$ bins. All the results are given in fig. 4.

These data can be compared to those of fig. 3. For protons the spin values issued from the kinetic energy distributions are higher than those estimated from the angular distributions.

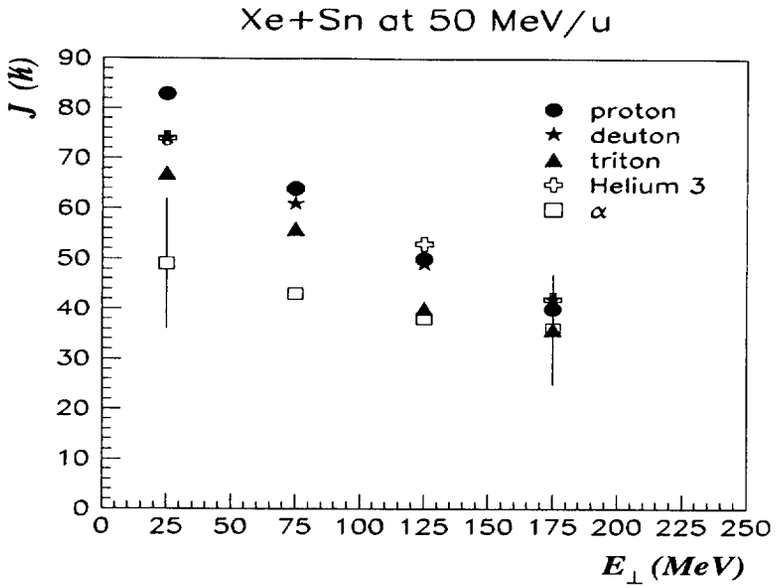


Figure 4: Idem as fig. 3 except that the apparent spin values are deduced from the kinetic energy spectra of LCP's (see text).

Moreover at the highest $E_\perp$ again the spin values determined with the kinetic energy are higher than those estimated from the angular distributions. From the data we know that the mid-velocity particles are preferentially emitted on the other side of the beam with respect to the PLF. Since the kinetic energy spectra of particles have been built by integrating all particles emitted in the forward hemisphere in the frame of the PLF, a contribution of mid-velocity particles is likely included which leads to a higher value for the spin. Limiting the integration domain to $0° < \Phi < 90°$ reduces the spin value by a factor 1.7 for $\alpha$ particle emission with $150 < E_\perp < 200$ MeV.

Meanwhile a qualitative agreement can be seen between the two sets of data (figs. 3 and 4) considering the large uncertainties.

# 5 Study of AMT as a function of $Z_{PLF}$ and $E_{bomb}$

An analysis of AMT has been done as a function of the atomic number of the detected PLF and as a function of the bombarding energy. Only protons and $\alpha$ particles have been looked for. The spin is extracted from the out-of-plane angular distributions integrated over the in-plane angle between -90° and 90° (the forward hemisphere of the PLF). We checked with the simulation that deriving the spin from the whole $W(\Theta,\Phi)$ angular distribution or from the $\Phi$ integrated $W(\Theta)$ distribution does not change significantly the results. They are given in fig. 5. The angular momentum decreases slightly with the decrease of the atomic number of the PLF, whatever the bombarding energy and the particle. Measurements done at 50 and 39 MeV/nucleon are very close from each other while larger values are observed at the lowest bombarding energy of 25 MeV/nucleon.

It should be noted that the experimental values obtained for PLF's very close to the projectile are higher than they should be: this is due to a wrong reconstruction of the

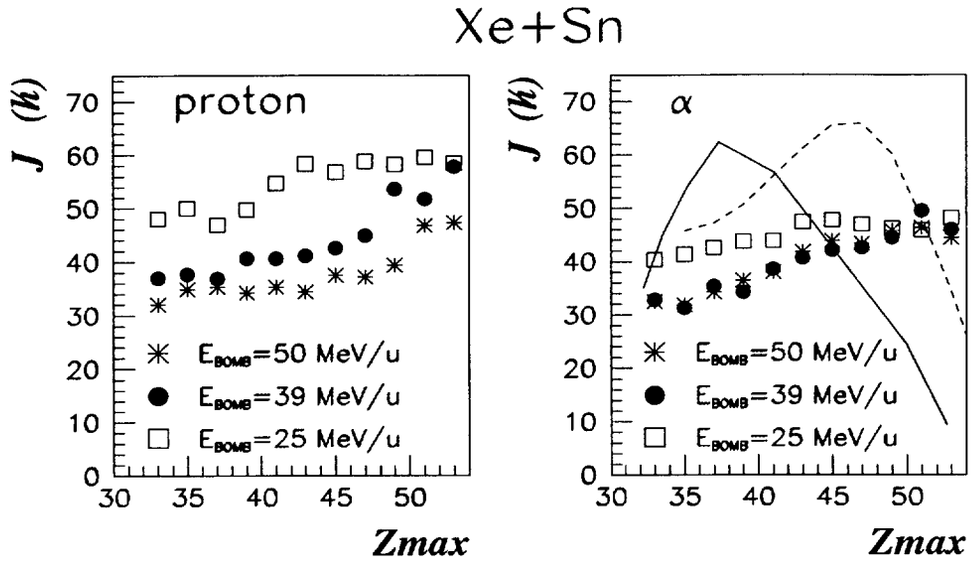


Figure 5: Apparent spin values extracted from angular distributions of protons and $\alpha$ particles as a function of the charge of the PLF and as a function of the bombarding energy. Solid and dashed lines correspond to the model predictions of refs. [6] and [23] at 25 MeV/nucleon, respectively.

reaction plane for these particular nuclei which have a low excitation energy.

# 6 Results and discussion

## 6.1 Apparent spin values

The spin values decrease strongly as a function of the transverse energy (see fig. 3). Such a decrease is unexpected as we should observe an increase of the spin with the increase of the $E_\perp$ transverse energy: in very peripheral collisions a small number of nucleon exchanges induces only very little angular momentum while in more dissipative collisions the larger number of exchanges should lead to higher spin values. The data are at variance with this expectation because they do not reflect the initial spin values of the PLF. They correspond to values averaged over the whole deexcitation chain undergone by the nucleus. In that sense they are apparent spin values in the same way as the slope parameter of a kinetic energy spectrum is an apparent temperature.

Estimation of the initial spin value of the PLF can only be performed doing simulation and applying the same procedure to the simulation as to the data. Nevertheless from the data shown in fig. 3 it well appears that $^3$He and to a lesser extent $^3$H are linked to higher spin values than the other particles, those particles (p, d and $\alpha$) leading to approximately the same values. From eq. 1 it is obvious that high spin values are connected to high temperature values. Nevertheless significantly larger spins are still deduced for $^3$He even if the same temperature is fixed for all LCP's in eq. 1.

## 6.2 Slope parameters and emission time

In table 1 are given for the different particles the slope parameters of the kinetic energy spectra measured along the spin axis in order to eliminate any influence of the angular momentum. Again the higher apparent temperatures are clearly associated to $^3$He nuclei, similar values are obtained for deuterons, tritons and $\alpha$ particles while protons have always the smallest values.

Coupling the results on the apparent spins and the apparent temperatures, we infer that $^3$He are likely emitted early in the deexcitation process in agreement with the observation done in the study of hot single sources in the $^{129}$Xe+$^{nat}$Sn central collisions at 50 MeV/nucleon [21].

| $E_\perp$ (MeV) | 0-50 | 50-100 | 100-150 | 150-200 |
|---|---|---|---|---|
| p | 3.2 | 3.8 | 4.1 | 4.7 |
| d | 4.4 | 4.9 | 5.2 | 6.2 |
| t | 3.7 | 4.3 | 5.3 | 6.1 |
| $^3$He | 5.8 | 6.5 | 8. | 8.6 |
| $\alpha$ | 3.8 | 4.8 | 5.7 | 6.1 |

Table 1: Slope parameters in MeV of the kinetic energy spectra of LCP's as a function of the $E_\perp$ transverse energy.

As for the other particles it is hard to see any hierarchy looking at both the apparent spin and temperature values. As a conclusion it is difficult to find any hierarchy in the emission time of the LCP's. It seems that these particles are emitted at any time. It is particularly surprising that $\alpha$ particles are not connected with the higher spin values as it is known from low energy statistical calculations [22]. Thereby the results of fig. 5 are not understood.

## 6.3 Comparison with model predictions

In the nucleon exchange transport (NET) model of Randrup [6] the energy and angular momentum are dissipated in the relative motion via the stochastic exchange of nucleons between the two partners during the interaction. In this model usual dynamical variables are taken into account as well as the three spin components of each nucleus which are explicitely introduced. No deexcitation step is included in the calculation, so in order to compare with the data, we assume that every evaporated nucleon carries away 13 MeV of excitation energy.

The second model, the Simon code of Durand [23], uses the same formalism to describe dynamically the interaction between the two ions. The statistical deexcitation of the nuclei is performed in a standard way with a time dependence for the emission of particles and fragments.

The spin values extracted from the data are compared to model predictions in fig. 5. Calculations have been done at the energy of 25 MeV/nucleon. The calculations correspond to the initial value of the spin of the PLF while the data are apparent values. Furthermore those data are minimum values as no spin fluctuations are included. Accounting for these facts a qualitative agreement can be deduced from the comparison, except for PLF's very

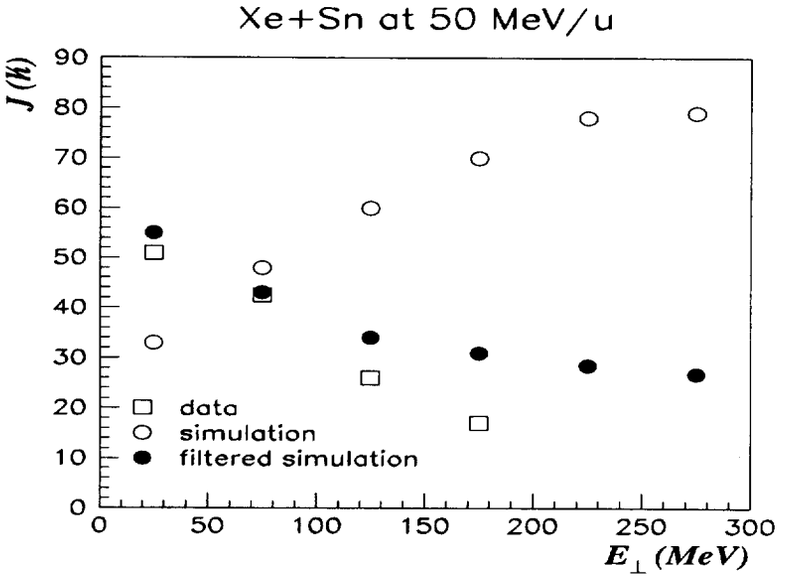


Figure 6: Apparent spin values extracted from the angular distributions of $\alpha$ particles. The data (open squares) are compared with the predictions of model of ref. [23] (full circles). The open circles represent the initial spin value of the PLF.

close to the projectile (cf. sect. 5). At 50 MeV/nucleon (not shown in the figure), the calculated spin values overestimate the data by nearly a factor 2. Particles emitted at velocities between those of the target and the projectile could explain this disagreement (see below).

In fig. 6 are displayed data already shown in fig. 3 together with the predictions of the Simon code [23]. Open circles represent the initial value of the spin of the PLF as a function of the transverse energy. As expected the spin value increases with the increase of the transverse energy. A meaningful comparison between data and model needs that simulated events be filtered by the experimental setup and analysed with the same procedure as the experimental data. This has been done for $\alpha$ particles (full circles in fig. 6). An excellent agreement is seen for peripheral collisions with $E_\perp < 100$ MeV. Above the discrepancy increases with the increase of the transverse energy. As we know the contribution of mid-velocity particles start to develop and the AMT may become less effective: either these particles waste a fraction of the initial spin or possibly the reaction mechanisms at intermediate bombarding energy (n-n collisions?) do not transfer as much spin as the one-body dissipation does at lower energy.

# 7 Conclusions

The amount of angular momentum imparted to the PLF in the $^{129}$Xe+$^{nat}$Sn reaction has been studied in peripheral collisions. The spin values have been extracted from the characteristics of LCP's: angular distributions and kinetic energy spectra. Both methods agree qualitatively.

The spin value is seen to decrease as a function of the violence of the collision (increase of the transverse energy or decrease of the detected PLF charge) . It has been shown that this

behaviour is linked to the average along the deexcitation chain of the PLF. Transport model calculations filtered by the experimental setup and analysed in the same way as the data describe nicely the most peripheral reactions. For these reactions the low energy concept of friction forces still apply, large spin values being transferred to the PLF. A discrepancy grows up with the energy dissipation which could be explained by the role of particles emitted at mid-velocity. This statement is reinforced by the fact that higher spin values are measured at 25 MeV/nucleon than at 50 MeV/nucleon. Particles emitted very early in the interaction take away a fraction of the initial orbital angular momentum leaving less angular momentum to be transferred to the residual nuclei, or dissipate a fraction of the intrinsic spins of these nuclei.

The study of AMT as a function of the atomic number of the PLF by means of the angular distributions of protons and $\alpha$ particles reveal some deviation with respect to low energy experiments. Indeed from the data it is difficult to conclude to any hierarchy in the emission times of LCP's.

# References


[1] R.A. Dayras *et al.*, Phys. Rev. **C22** (1980) 1485.

[2] R. Babinet *et al.*, Z. Phys. **A295** (1980) 153.

[3] J.C. Steckmeyer *et al.*, Nucl. Phys. **A427** (1984) 357.

[4] M. Lefort and C. Ngô, Ann. de Phys. **3** (1978) 5.

[5] L.G. Moretto and R.P. Schmitt, Phys. Rev. **C21** (1980) 204.

[6] J. Randrup, Nucl. Phys. **A383** (1983) 468.

[7] W. Trautmann *et al.*, in Proceedings of the XXXI$^{st}$ International Winter Meeting on Nuclear Physics, Bormio, Italy, ed. I. Iori (Univ. di Milano, Milano, 1993).

[8] J. Colin *et al.*, Nucl. Phys. **A593** (1995) 48 and references therein.

[9] R. Broglia *et al.*, Phys. Rev. Lett. **41** (1978) 25.

[10] D.P. Min, J. Phys. **C401** (1978) 431.

[11] W. Cassing, Z. Phys. **A327** (1987) 447.

[12] G.F. Bertsch, Z. Phys. **A289** (1978) 103.

[13] A. Botvina and D.H.E. Gross, Nucl. Phys. **A592** (1995) 257.

[14] J. Pouthas *et al.*, Nucl. Instr. and Meth. **A357** (1995) 418 and *ibid* **A369** (1996) 222.

[15] J.C. Steckmeyer *et al.*, Nucl. Instr. and Meth. **A361** (1996) 472.

[16] J. Lukasik *et al.*, Phys. Rev. **C55** (1997) 1906.

[17] J. Péter *et al.*, Nucl. Phys. **A593** (1993) 95.

[18] J.C. Steckmeyer *et al.*, Phys. Rev. Lett. **76** (1996) 4895.

[19] E. Genouin-Duhamel, Thesis, Caen 1999.

[20] N.N. Ajitanand *et al.*, Phys. Rev. **C34** (1986) 877.

[21] N. Marie *et al.*, Phys. Lett. **B391** (1997) 15.

[22] R.C. Reedy *et al.*, Phys. Rev. **188** (1969) 1771.

[23] D. Durand, Nucl. Phys. **A541** (1992) 266 and D. Durand *et al.*, in preparation.